



J. Serb. Chem. Soc. 85 (1) 53–66 (2020)
JSCS–5282

Journal of
the Serbian
Chemical Society

JSCS-info@shd.org.rs • www.shd.org.rs/JSCS

UDC 547.835.5:547.461.4+519.677+543.422:
615.004.12

Original scientific paper

Spectroscopic (FTIR, UV–Vis and NMR), theoretical investigation and molecular docking of substituted 1,8-dioxodecahydroacridine derivatives

KRISHNA KANT YADAV¹, ABHISHEK KUMAR¹, SANCHARI BEGAM²,
KHONDEKAR NURJAMAL², AMARENDRA KUMAR^{1*}, GOUTAM BRAHMACHARI²
and NEERAJ MISRA¹

¹Department of Physics, University of Lucknow, Lucknow-226007, India and ²Laboratory of Natural Products & Organic Synthesis, Department of Chemistry, Visva-Bharati (a Central University), Santiniketan-731 235, West Bengal, India

(Received 28 December 2018, revised 6 September, accepted 16 September 2019)

Abstract: Recently, substituted 1,8-dioxodecahydroacridine derivatives have been investigated and found to possess a wide variety of biological and pharmacological activities. Two of these biologically relevant *N*-heterocyclic scaffolds, 2-(9-(4-methoxyphenyl)-3,3,6,6-tetramethyl-1,8-dioxo-1,2,3,4,5,6,7,8-octahydroacridin-10(9*H*)-yl)succinic acid (MTDOSA) and 2-(3,3,6,6-tetramethyl-9-(4-nitrophenyl)-1,8-dioxo-1,2,3,4,5,6,7,8-octahydroacridin-10(9*H*)-yl)-succinic acid (NTDOSA), have been studied in ground and first excited state using DFT method employing B3LYP/6-311++G(d,p) level of theory. Quantum chemical calculations of geometrical structure and vibrational wave-numbers of MTDOSA and NTDOSA were carried out using DFT method. The experimental FT-IR spectra of the compounds were recorded in the range 4000–400 cm⁻¹ and comprehensively interpreted on the basis of potential energy distribution. The global reactivity descriptors are calculated and discussed. Moreover, ¹H- and ¹³C-NMR spectral data have been calculated using the gauge independent atomic orbital method and compared with experimental spectra. The docking studies reveal that the compounds MTDOSA and NTDOSA have strong binding affinity toward the target protein 5KLH. Thus, the compounds have a possible use as an antileishmanial drug.

Keywords: quantum chemical study; spectroscopy; global reactivity descriptors; antileishmanial drug.

INTRODUCTION

Diversely substituted 1,8-dioxodecahydroacridine derivatives have been studied for their wide range of notable pharmacological properties including antima-

*Corresponding author. E-mail: akgkp25@yahoo.co.in
<https://doi.org/10.2298/JSC181228102Y>



larial, antitumor, antiprion, anti-Alzheimer's, antimicrobial, antileishmanial and antitrypanosomal¹⁻³ activities in the last decade. Positive ionotropic tropic effects have been exhibited by acridines⁴ and its derivatives such as 1,8-dioxo-decahydroacridines are also recognized as laser dyes.⁵ Having wide range of applicability, various synthetic procedures have been adapted to generate these biologically important compounds and their derivatives.^{6,7} Brahmachari *et al.*⁸ recently reported a simple and convenient, eco-friendly, low-cost and practical protocol for the synthesis of a new series of diversely substituted 1,8-dioxo-decahydroacridines, particularly bearing various amino acids as part of the building block. Keeping diverse biological and pharmacological properties of substituted 1,8-dioxodecahydroacridine derivatives in mind, herein we are presenting a detailed comparative study of geometric and electronic structure of 2-(9-(4-methoxyphenyl)-3,3,6,6-tetramethyl-1,8-dioxo-1,2,3,4,5,6,7,8-octahydroacridin-10(9*H*)-yl)succinic acid (MTDOSA) and 2-(3,3,6,6-tetramethyl-9-(4-nitrophenyl)-1,8-dioxo-1,2,3,4,5,6,7,8-octahydroacridin-10(9*H*)-yl)succinic acid (NTDOSA) in ground and first excited state is presented. The experimental spectral data (FT-IR, UV and NMR) of MTDOSA and NTDOSA are compared with the data calculated using theoretical (DFT/B3LYP) method. The molecular properties such as dipole moment, molecular electrostatic potential surfaces and frontier orbital band gap energies have been calculated for the better understanding of the properties of both compounds. Since the compounds under consideration are substituted derivatives of a biologically and pharmacologically active moiety, global reactivity descriptors like chemical potential, electronegativity, hardness, softness and electrophilicity index have been calculated and used to predict the reactivity of the molecules.

EXPERIMENTAL

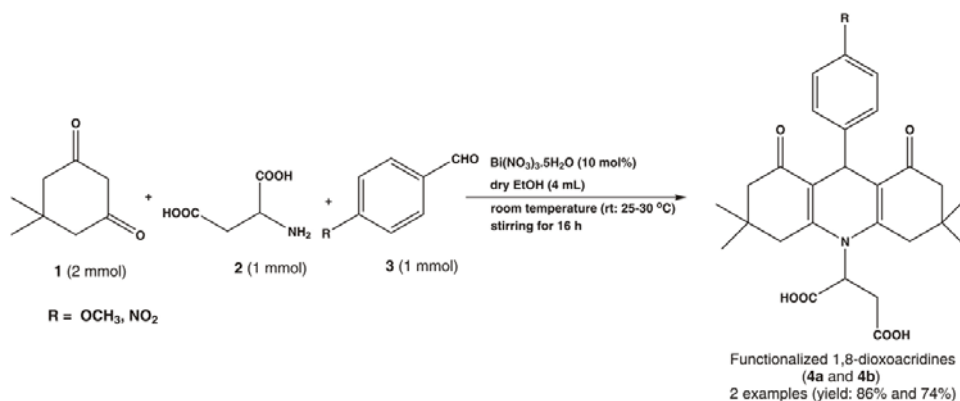
The FT-IR spectrum of title molecules were recorded between 4000–400 cm^{-1} on a Shimadzu (FT-IR 8400S) FT-IR spectrophotometer using KBr disc. UV-Vis spectra for MTDOSA and NTDOSA were measured on a Shimadzu UV-1800 spectrophotometer with 1 cm quartz cell optical path length using MeOH as solvent, with their respective concentration of 2.02×10^{-4} and 1.96×10^{-4} mol L^{-1} . Their ^1H - and ^{13}C -NMR spectra were obtained at 400 and 100 MHz, respectively, using Bruker DRX-400 spectrometer and $\text{DMSO}-d_6$ as the solvents. Solvents were purchased from Sigma Aldrich.

Analytical and spectral data of the compounds are given in Supplementary material to this paper.

General procedure for the synthesis of substituted 1,8-dioxoacridines 4a and b

The title compounds were synthesized following the methodology previously published (Scheme 1).⁸ Dimedone (**1**; 1 mmol), aspartic acid (**2**; 1 mmol), $\text{Bi}(\text{NO}_3)_3 \cdot 5\text{H}_2\text{O}$ (10 mol%; 49 mg) and 4 mL dry ethanol were transferred to an oven-dried sealed tube in a sequential manner at ambient conditions, and the reaction mixture was then stirred vigorously for about 2 h. Afterwards, another portion of dimedone (**1**; 1 mmol) and 4-methoxybenzaldehyde (**3a**, 1 mmol)/4-nitrobenzaldehyde (**3b**, 1 mmol) was added to the stirred reaction mixture, and the

stirring was continued for up to next 14 h under same reaction conditions. The progress of the reaction was monitored by TLC. On completion of the reaction, a solid mass precipitated out which was filtered off, followed by purification of the crude product by recrystallization from ethanol to furnish pure product **4a** and **b** (Fig. 1). The structure of each of the products was confirmed by analytical as well as spectral studies including FT-IR, $^1\text{H-NMR}$, $^{13}\text{C-NMR}$ and DEPT-135. The characterization data of the synthesized compounds **4a** and **b** are given in as supplementary material.



Scheme 1. Bismuth nitrate-catalyzed one-pot synthesis of substituted 1,8-dioxoacridines (**4a** and **b**) at ambient conditions.

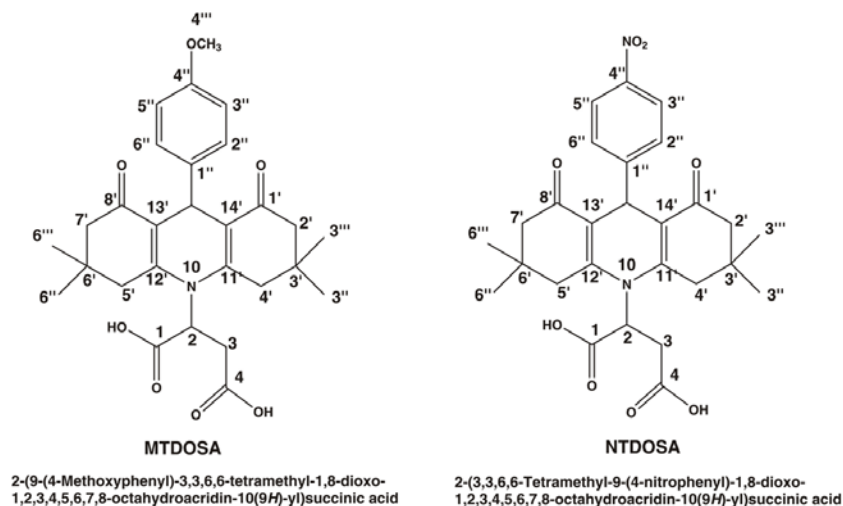


Fig. 1. Chemical structures of MTDOA and NTDOA.

Computational details

All computations herein were executed using the GAUSSIAN-09 program package.⁹ B3LYP of DFT and 6-311++G (d,p) basis set was used throughout the calculations. The vibrational unscaled wavenumbers we calculated and scaled down by the appropriate factor.^{10,11}

The vibrational wavenumber assignments have been carried out by the corresponding potential energy distributions (PEDs) and the PEDs we computed from the VEDA 4 program.¹² TD-DFT calculations were performed in conjugation with IEFPCM model for solvent effect in methanol. ¹H- and ¹³C-NMR chemical shifts of title compound were obtained using including atomic orbital (GIAO) method in DMSO at DFT/B3LYP method with 6-311++G(d,p) basis set.

RESULTS AND DISCUSSION

Molecular geometry

The geometry optimization for both molecules has been achieved by energy minimization, using DFT at the B3LYP level with 6-311++G(d,p) basis set. Optimized geometry of the molecules was further ensured to be located at the local true minima on potential energy surface, because calculated vibrational spectra contain no imaginary wavenumber. The calculated optimized geometrical parameters (bond lengths, bond angles and dihedral angles) of the MTDOSA and NTDOA molecules are listed in Tables S-I and S-II of the Supplementary material, respectively, and the optimized molecular structures thus obtained along with the numbering scheme of the atoms are depicted in Fig. 2. In the six-membered rings (R₁–R₄) of molecules MTDOSA/NTDOA, all the C–C bonds, N–C bond and C–H bond lengths are in full agreement with those reported in literature.¹³ In both the molecules C=O bond lengths are equal to 1.221 Å, close to the standard C=O bond length (1.220 Å).^{13,14}

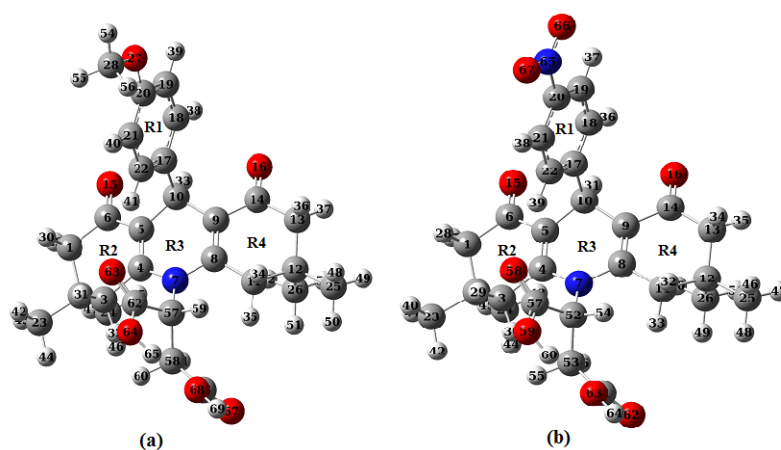


Fig. 2. The optimized geometric structure of MTDOSA (a) and NTDOA (b) molecule.

In both the molecules (MTDOA /NTDOA), the fused rings R2, R3 and R4 are showing some non-planarity, as evident from the dihedrals involved ($C1-C6-C5-C10 = 173.02^\circ/174.38^\circ$ and $C10-C9-C14-C13 = 172.14^\circ/173.41^\circ$). The dihedrals $C5-C10-C17-C12$ ($41.44^\circ/41.97^\circ$) and $C9-C10-C17-C18$ ($96.70^\circ/97.11^\circ$) show non-planarity of ring R1 with ring R3.

Vibrational analysis and FTIR spectrum

The theoretical vibrational analysis of both molecules were performed by using B3LYP level with 6-311++G (d,p) basis set. The experimental and calculated vibrational wavenumbers of MTDOSA and NTDOSAs, along with their PED, are given in Tables S-III and S-IV of the Supplementary material, respectively. The calculated harmonic wavenumbers are generally slightly higher than that of their experimental counterpart. Therefore, proper scaling factors^{10, 11} are employed to have a better agreement with the experimental wavenumbers. In the present study, vibrational wavenumbers calculated at B3LYP/6-311++G (d,p) level have been scaled by 0.967. The calculated IR spectrum of both the molecules agree well with the recorded FT-IR spectra in the region 4000–400 cm^{-1} using samples in the form of KBr disc. The experimental FT-IR and theoretical IR spectra of MTDOSA and NTDOSAs have been shown in Fig. 3. It should be mentioned herein that the FT-IR absorption peaks around 2360 cm^{-1} (experimental error and not characteristics of the chemical structures of the title molecules), recorded in both the spectra, are due to the atmospheric carbon dioxide encapsulated within the pores of the walls of KBr disc during sample preparation.

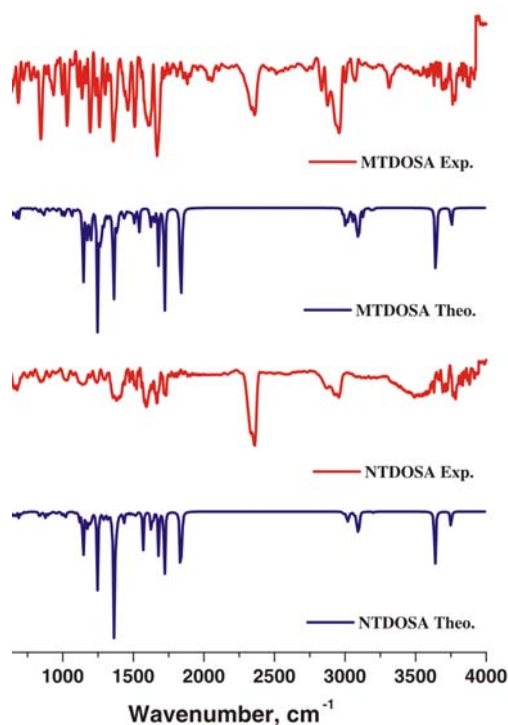


Fig. 3. The calculated IR and experimental FTIR spectra of MTDOSA and NTDOSAs molecule.

O–H vibrations

Generally, the O–H stretching vibrations are found to be in the region around 3500 cm^{-1} .¹⁵ In case of MTDOSA/NTDOSA the calculated stretching modes are found at $3629/3627$ and $3523/3517\text{ cm}^{-1}$. The O–H in-plane bending vibration, in general lies in the region $1250\text{--}1150\text{ cm}^{-1}$.¹⁵ In the present molecular study of MTDOSA/NTDOSA, the O–H in-plane bending vibration appears as a weak band in both molecules in the range $1275\text{--}1316/1253\text{--}1316\text{ cm}^{-1}$.

Ring vibrations

In case of aromatic compounds multiple weak bands are generally observed in the range $3100\text{--}3000\text{ cm}^{-1}$.¹⁶ These bands are due to aromatic C–H stretching vibrations. In the present study, in case of MTDOSA and NTDOSA, both having three rings fused with each other and one phenyl ring, very weak bands in this region of the FT-IR spectra are shown. The symmetric and asymmetric C–H stretching modes of MTDOSA/NTDOSA, calculated at $3097/3115$, $3090/3094$, $3083/3093$, $3001/3002$, $2981/2983$ and $2960/2962\text{ cm}^{-1}$, are assigned well with FT-IR spectra.

C=O vibration

In IR spectra the appearance of a band around 1700 cm^{-1} shows the presence of a carbonyl group and is due to the C=O stretching. In the present study, the asymmetric stretching modes of C=O groups are calculated at higher wavenumbers ($1785/1784\text{ cm}^{-1}$) and the symmetric stretching modes of C=O at slightly lower wavenumbers ($1660/1659\text{ cm}^{-1}$) for MTDOSA/NTDOSA.

CH₃ vibrations

Both compounds (MTDOSA/NTDOSA) have four methyl groups attached to the ring (R2 and R4). The anti-symmetric and symmetric C–H stretching mode of the CH₃ group is expected around 2980 and 2870 cm^{-1} respectively. The asymmetric C–H stretching vibrational modes of CH₃ are calculated at 2987 , 2983 , 2975 , 2974 cm^{-1} and 2997 , 2989 , 2988 , 2984 cm^{-1} for MTDOSA and NTDOSA molecules respectively. Symmetric CH₃ stretching modes for MTDOSA and NTDOSA molecules are calculated at 2926 , 2923 and 2978 , 2975 cm^{-1} , respectively. The bending mode of vibrations of methyl group appears within the region $1465\text{--}1440\text{ cm}^{-1}$. In the present investigation the wavenumbers corresponding to CH₃ bending vibration are ranged from 1464 to 1456 cm^{-1} in both molecules.

UV–Vis analysis

Ultraviolet spectral analyses of MTDOSA and NTDOSA molecules have been performed by experimental and TD-DFT/B3LYP/6-311++G (d,p) method. The electronic spectra have been recorded in methanol at room temperature. The

calculated absorption wavelengths, (nm), oscillator strengths (f) and vertical excitation energies (E) in methanol solution phase were carried out and compared with experimental values (Tables S-V and S-VI of the Supplementary material). The comparative experimental and theoretical UV–Vis spectrum of MTDOSA and NTDOSA has been given in Fig. 4.

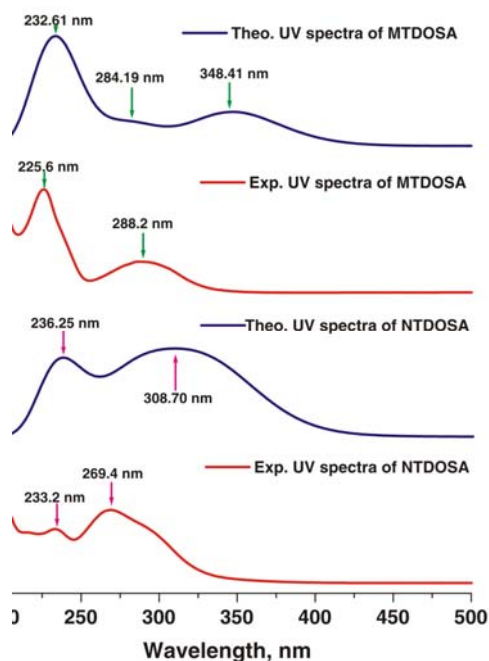


Fig. 4. Recorded and calculated UV-spectra of MTDOSA and NTDOSA in methanol solvent.

One can note that there are two intense peaks observed at 288.2 and 225.6 nm in experimental spectra of MTDOSA in methanol, which are assigned to a shoulder at 284.19 and a peak at 232.61 nm in calculated spectra. Another peak at 348.41 nm has also been observed in theoretical UV spectra. These absorption maxima at 284.19, 232.61 and 348.41 nm are due to electronic transition from HOMO→LUMO+1, HOMO–4→LUMO+1 and HOMO–1→LUMO. In the case of NTDOSA, the calculated absorption maxima at 236.25 nm corresponds to the electronic transition HOMO→LUMO+7 and is in good agreement with the experimental absorption peak at 233.2 nm.

NMR analysis

Nuclear magnetic resonance (NMR) spectroscopy provides detailed information about the electronic structure and is an important tool to probe the surroundings of a nucleus. Carbon and hydrogen shielding tensors of MTDOSA and NTDOSA molecules are studied using both experimental and theoretical techni-

ques. The experimental ^1H - and ^{13}C -NMR spectra of MTDOSA and NTDOSA are given in Figs. S-1–S-8 of the Supplementary material. ^1H - and ^{13}C -NMR chemical shifts of the title molecules were calculated with the optimized molecular structure at DFT-B3LYP/6-311++G (d,p) level using the GIAO method with TMS as a reference. The values of experimental chemical shift, along with the calculated chemical shifts of molecules under consideration, are listed in Tables S-VII and S-VIII of the Supplementary material.

Generally, the aromatic carbon shows chemical shift values from 100 to 150 ppm in ^{13}C -NMR spectrum. The chemical shifts of carbon atoms of ring (R1) in MTDOSA were calculated in the range 114.61–167.59 ppm with the experimental recorded value from 129.40 to 158.06 ppm in DMSO. This is due to the presence of electron-donating group MeO, which increased shielding in *ortho* positions. Due to the presence of electron withdrawing group NO_2 , which also increases deshielding, the molecule NTDOSA shows the chemical shift of carbon in range 130.07–164.77 ppm, which is in agreement with experimental value.

In the ring R2 and R4 chemical shift of ^{13}C -NMR vary in the range 42.68–205.96/42.42–206.23 ppm and experimentally recorded values vary between 31.05–196.62/39.38–182.51 ppm in MTDOSA/NTDOSA. The C6 and C14 atoms have larger chemical shifts (205.96/205.92 and 205.93/206.23 ppm) than the other ring carbon atoms, due to de-shielding effect of the electronegative oxygen atom. Due to the presence of the electronegative nitrogen atoms in ring R3, the C4 and C8 atom get de-shielded and hence correspond to nuclear magnetic resonances of higher frequencies. The carbon atoms C62, C66 in MTDOSA and C53, C57 in NTDOSA in carboxylic group get de-shielded due to the presence of two electronegative oxygen atoms, hence the carboxylic group shows chemical shift at higher value.

^1H -NMR chemical shift of MTDOSA/NTDOSA show the presence of singlet in the range 0.81–1.36/0.82–1.36 ppm for protons of methyl group attached to the ring and experimental chemical shifts of ^1H -NMR spectrum of these protons in DMSO solvent are in range of 0.97–1.08/1.83–2.25 ppm. The calculated doublet chemical shift of MTDOSA/NTDOSA ranges from 6.90–8.12/8.10–8.48 ppm corresponding to the proton attached with ring R1. The ^1H -NMR chemical shift of proton attached with ring R2 and R4 shows presence of a multiplet band in the range 1.86–2.95/1.91–2.91 ppm of MTDOSA/NTDOSA. A singlet at δ 5.35/5.50 ppm corresponds to protons directly attached to R3 of MTDOSA/NTDOSA. In the molecule MTDOSA a singlet is obtained in the range 3.76–4.11 ppm and it corresponds to protons of methyl group directly attached to the oxygen attached with R1.

Electronic parameters

Frontier molecular orbitals, namely highest occupied molecular orbital (HOMO) and lowest unoccupied molecular orbital (LUMO) determine the way the molecule interacts with other species. The energy difference between HOMO and LUMO can be used to predict the chemical reactivity and kinetic stability of a molecule. A molecule with a small frontier orbital gap indicates its polarizable nature and is generally associated with a high chemical reactivity, low kinetic stability and such a molecule is termed as soft molecule. In the present DFT study, the frontier orbital gaps in case of MTDOSA and NTDOSA are 3.899 and 4.012 eV, respectively, *i.e.*, the frontier orbital gap in MTDOSA is 0.113 eV lower than NTDOSA. The 3D plots of HOMO and LUMO frontier molecular orbitals for both molecules are shown in Fig. S-3. In the compound MTDOSA, HOMO is found to be distributed mostly over the entire compound, except the phenyl ring (R1) and the methoxy group, while the LUMO is mostly contributed by methoxy phenyl ring with a small involvement of the entire fused heterocyclic ring, but in case of NTDOSA the contribution of HOMO is over the nitrophenyl ring (R1) and a little involvement of all fused heterocyclic rings, whereas LUMO is distributed over the whole molecule except nitrophenyl ring.

Electronic chemical potential (μ), absolute hardness (η) and global electrophilicity index (ω)^{17,18} are the descriptors of molecular stability and reactivity. These universal concepts may be defined using DFT. According to Parr¹⁹ and Pearson,²⁰ μ (which is equal to the negative of the electronegativity of atoms and molecules) was defined as:

$$\mu = -1/2(I + A) \quad (1)$$

where I is the vertical ionization energy and A stands for the vertical electron affinity. Absolute hardness can be shown to be:¹⁷⁻²²

$$\eta = I - A \quad (2)$$

Furthermore, ω was introduced by Parr^{17,23,24} and may be obtained using μ and η :

$$\omega = \frac{\mu^2}{2\eta} \quad (3)$$

The parameter ω defines the capability of a species to accept electrons. Thus, the low value of ω has been associated with a good nucleophile, while a high value of it characterizes a good electrophile. This new reactivity property has been manifested recently in explaining the toxicity of various pollutants in terms of their reactivity and site selectivity.²⁵ The calculated values of the global reactivity parameters for the MTDOSA and NTDOSA molecules have been reported in Table I. The substituted acridine derivative MTDOSA contains donor substituent methoxyphenyl that increases the energy of the HOMO and of the

LUMO, while NTDOSA contains the acceptor substituent nitrophenyl which decreases the energy of HOMO and LUMO. The energy gap in MTDOSA (3.899 eV) is lower than NTDOSA (4.012 eV) and it that reveals MTDOSA is more reactive in comparison to NTDOSA. The high value of chemical potential (-3.7149 eV) and the low value of electrophilicity index (1.7694 eV) for MTDOSA characterizes its electrophilic behaviour, while compound NTDOSA having lower value of chemical potential (-4.4405 eV) and higher value of electrophilicity index (2.4567 eV) makes its character nucleophilic.

TABLE I. Electronic parameters of MTDOSA and NTDOSA at B3LYP/6311++ G (d,p)

Reactivity descriptor	DFT/B3LYP/6311++G(d,p)	
	MTDOSA	NTDOSA
I / eV	5.6647	6.4470
A / eV	1.7651	2.4348
η / eV	3.8996	4.013
μ / eV	-3.7149	-4.4405
ω / eV	1.7694	2.4567

Molecular electrostatic potential

The molecular electrostatic potential (MEP) and electronic density are related to each other and the MEP yields information on the molecular regions, which are preferred or avoided by an electrophile or nucleophile. MEP is a very useful parameter for determining reactive sites in the molecular system.²⁶ The electrostatic potential increases by different colours in the order of red < orange < yellow < green < blue. The maximum negative region indicated by red colour represents the site for electrophilic attack, while the regions of nucleophilic attack are indicated by blue colour and represent a maximum positive region.^{27,28} MEPs for both the molecules were plotted using B3LYP/6-311++G (d,p) level for the optimized geometry, to predict the reactive sites for electrophilic and nucleophilic attack, are shown in Fig. S-10. From the MEP map of MTDOSA it can be seen that the region of negative potential is over the oxygen atom and the region having positive potential is over the hydrogen atoms of the fused rings. In case of NTDOSA the most negative potential region is hovering over nitro group and all the oxygen.

Molecular docking

The molecular docking reveals the process by which a drug (molecule) and a receptor fit together and dock to each other well, and the molecule binding to a receptor inhibits its function and thus acts effectively as a drug. The docking was done by Swiss Dock²⁹ which avoids sampling bias and provides a way of docking over whole protein without specifying the region of the protein as a bonding pocket. The resulting output clusters were obtained after each run and the result

for both compounds shows that cluster 0 is having the best full fitness (FF) score. The more favourable binding site between a ligand and its receptor is signified by the highest negative FF score. On account of antileishmanial activities shown by substituted 1,8-dioxodecahydroacridine derivative, the docking studies have been performed on the title compounds, MTDOSA and NTDOSA with *Trypanosoma brucei* pro-cyclic specific surface antigen-2 (TbPSSA-2, PDB ID: 5KLH),³⁰ the reason for the vector-borne diseases of humans and livestock in sub-Saharan Africa. The FF score obtained for protein targets clearly shows that the molecule MTDOSA is bonded with the target protein with one hydrogen bond at 2.583 Å (FF score: -1466.9 kcal*/mol and binding affinity ΔG : -7.57 kcal/mol) and NTDOSA are effectively bonded with 5KLH target with four hydrogen bonds at 2.030, 2.036, 2.295 and 2.355 Å, respectively (FF score: -1459.1 kcal/mol and binding affinity ΔG : -7.86 kcal/mol). The docking picture obtained from the UCSF chimera software³¹ is shown in Fig. 5. The docking result suggests that the title compounds have strong binding affinity towards the target protein, achieving the best FF score against 5KLH. Thus, the compounds might be used as active agents for transmission blocking therapy against TbPSSA-2.

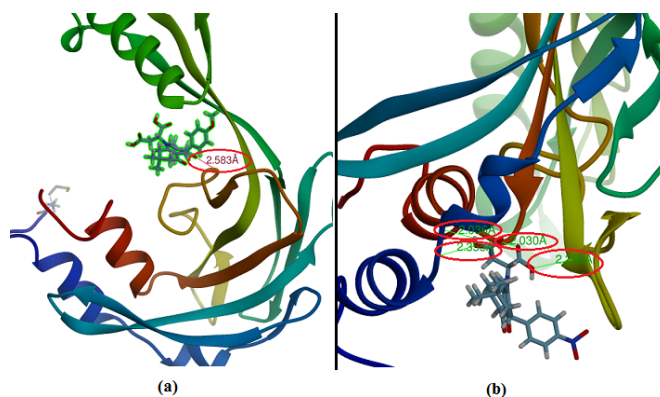


Fig. 5. Hydrogen bond interaction of MTDOSA (a) and NTDOSA (b) with 5KLH.

CONCLUSIONS

The experimental (FT-IR, NMR and UV-Vis techniques) and theoretical quantum chemical method have been employed to analyze the spectroscopic properties of MTDOSA and NTDOSA. The optimized geometric parameters and vibrational harmonic wavenumbers of the compounds have been calculated using DFT/B3LYP methods with 6-311++G (d,p) basis set. A good agreement between the experimental and the calculated normal modes of vibrations has been found and vibrational modes are successfully assigned using the potential energy distribution. The calculated UV-Vis absorption peaks in methanol of both the

* 1 kcal = 4184 J

compounds match well with the experimentally observed absorption peaks. The calculated global reactivity parameters reveal that the compound NTDOSA is a good nucleophile while the compound MTDOSA is a good electrophile. The molecular docking results show that the compounds MTDOSA and NTDOSA have strong binding affinity toward the target protein 5KLH. Thus, the compounds may be used as an antileishmanial drug.

SUPPLEMENTARY MATERIAL

Characterization data of the synthesized compounds **4a** and **b** are available electronically from <http://www.shd.org.rs/JSCS/>, or from the corresponding author on request. The recorded ¹³C- and ¹H-NMR spectra of NTDOSA and MTDOSA in DMSO solution are shown in Figs. S-1–S-8. The HOMO–LUMO plots and MESP for both the molecules are shown in Figs. S-9 and S-10, respectively. The optimized geometric parameters for compounds MTDOSA and NTDOSA are listed in Tables S-I and S-II, respectively. The vibrational analyses of prominent modes of the title compounds along with the experimental data are given in Tables S-III and S-IV. The experimental and the calculated absorption wavelengths, the excitation energies, the absorbance values and the oscillator strengths of the MTDOSA and NTDOSA molecules are given in Tables S-V and S-VI, respectively. The calculated and the experimentally observed values of ¹H and ¹³C chemical shifts of MTDOSA and NTDOSA, for the proton and for carbon atoms in DMSO solvent, taking tetramethylsilane (TMS) as a reference, are depicted in Tables S-V and S-VI, respectively.

ИЗВОД

СПЕКТРОСКОПИЈА (FTIR, UV–Vis И NMR), ТЕОРИЈСКО ИСТРАЖИВАЊЕ И МОЛЕКУЛСКИ ДОКИНГ СУПСТИТУИСАНИХ ДЕРИВАТА 1,8-ДИОКСОДЕКАХИДРОАКРИДИНА

KRISHNA KANT YADAV¹, ABHISHEK KUMAR¹, SANCHARI BEGAM², KHONDEKAR NURJAMAL², AMARENDRA KUMAR¹, GOUTAM BRAHMACHARI² И NEERAJ MISRA¹

¹Department of Physics, University of Lucknow, Lucknow-226007, India и ²Laboratory of Natural Products & Organic Synthesis, Department of Chemistry, Visva-Bharati (a Central University), Santiniketan-731 235, West Bengal, India

Супституисани деривати 1,8-диоксодекахидроакридина су недавно истраживани и нађено је да имају разноврсне биолошке и фармаколошке активности. Два од ових биолошки релевантних *N*-хетероцикличних скелета 2-(9-(4-метоксифенил)-3,3,6,6-тетраметил-1,8-диоксо-1,2,3,4,5,6,7,8-октахидро-акридин-10(9*H*)-ил)ћилибарна киселина (MTDOSA) и 2-(3,3,6,6-тетраметил-9-(4-нитрофенил)-1,8-диоксо-1,2,3,4,5,6,7,8-октахидроакридин-10(9*H*)-ил)ћилибарна киселина (NTDOSA) проучавани су у основном и првом ексцитованом стању користећи DFT метод на B3LYP/6-311++G (d,p) нивоу теорије. Квантохемијска израчунавања геометрије структура и вибрационих таласних бројева за MTDOSA и NTDOSA изведена су користећи DFT метод. Експериментални FT-IR спектри једињења су снимљени у области 4000–400 cm⁻¹ и свеобухватно су тумачени на основу расподеле потенцијалне енергије. Глобални дескриптори реактивности су израчунати и дискутовани. Надаље, израчунати су ¹H- и ¹³C-NMR спектрални подаци користећи GIAO метод и упоређени су са експерименталним спектрима. Студија доковања показује да једињења MTDOSA и NTDOSA имају јак афинитет везивања за циљни протеин 5KLH. Тако, једињења могу имати примену као лек за лишманијазу.

(Примљено 28. децембра 2018, ревидирано 6. септембра, прихваћено 16. септембра 2019)

REFERENCES

1. C. Santelli-Rouvier, B. Pradines, M. Berthelot, D. Parzy, J. Barbe, *Eur. J. Med. Chem.* **39** (2004) 735 (<https://dx.doi.org/10.1016/j.ejmech.2004.05.007>)
2. T. L. Su, Y. W. Lin, T. C. Chou, X. Zhang, V. A. Bacherikov, C. H. Chen, L. F. Liu, T. J. Tsai, *J. Med. Chem.* **49** (2006) 3710 (<https://dx.doi.org/10.1021/jm060197r>)
3. S. A. Gamage, D. P. Figgitt, S. J. Wojcik, R. K. Ralph, A. Ransijn, J. Mauel, V. Yardley, D. Snowdon, S. L. Croft, W. A. Denny, *J. Med. Chem.* **40** (1997) 2634 (<https://dx.doi.org/10.1021/jm970232h>)
4. R. A. Janis, D. J. Triggle, *J. Med. Chem.* **26** (1983) 775 (<https://dx.doi.org/10.1021/jm00360a001>)
5. M. Kaya, Y. Yıldırım, L. Terker, *J. Heterocycl. Chem.* **46** (2009) 294 (<https://dx.doi.org/10.1002/jhet.45>)
6. X.-S. Wang, M.-M. Zhang, Z.-S. Zeng, D.-Q. Shi, S.-J. Tu, X.-Y. Wei, Z.-M. Zong, *Tetrahedron Lett.* **46** (2005) 7169 (<https://dx.doi.org/10.1016/j.tetlet.2005.08.091>)
7. B. Banerjee, G. Brahmachari, *J. Chem. Res.* **38** (2014) 745 (<https://dx.doi.org/10.3184/174751914X14177132210020>)
8. G. Brahmachari, S. Begam, K. Nurjamal, *ChemistrySelect* **2** (2017) 331 (<https://dx.doi.org/10.1002/slct.201700265>)
9. Gaussian 09, Revision A.1, Gaussian, Inc., Wallingford CT, 2009
10. A. P. Scott, L. Radom, *J. Phys. Chem.* **100** (1996) 16502 (<https://dx.doi.org/10.1021/jp960976r>)
11. P. Pulay, G. Fogarasi, G. Pongor, J. E. Boggs, A. Vargha, *J. Am. Chem. Soc.* **105** (1983) 7037 (<https://dx.doi.org/10.1021/ja00362a005>)
12. M. H. Jamroz, *Spectrochim. Acta, A* **114** (2013) 220 (<https://doi.org/10.1016/j.saa.2013.05.096>)
13. M. Ladd, *Introduction to Physical Chemistry*, 3rd ed., Cambridge University Press, Cambridge, 1998 (ISBN 0521480000)
14. F. H. Allen, O. Kennard, D. G. Watson, L. Brammer, A. G. Orpen, R. Taylor, *J. Chem. Soc., Perkin Trans.* **2-12** (1987) S1 (<https://dx.doi.org/10.1039/P2987000005I>)
15. D. Michalska, D. C. Bienko, A.J. Abkowicz-Bienko, Z. Latajaka, *J. Phys. Chem.* **100** (1996) 17786 (<https://dx.doi.org/10.1021/jp961376v>)
16. R. L. Pecsok, L. D. Shield, I. C. McWilliam, *Modern Methods of Chemical Analysis*, Wiley, New York, 1976 (ISBN 10: 0471676624/ISBN 13: 9780471676621)
17. P. K. Chattaraj, U. Sarkar, D.R. Roy, *Chem. Rev.* **106** (2006) 2065 (<https://dx.doi.org/10.1021/cr040109f>)
18. P. A. Johnson, L. J. P. Bartolotti, W. Ayers, T. Fievez, P. Geerlings, in *Modern Charge Density Analysis*, C. Gatti, P. Macchi Eds., Springer, New York, 2012 (https://dx.doi.org/10.1007/978-90-481-3836-4_21)
19. R. G. Parr, R. A. Donnelly, M. Levy, W. E. Palke, *J. Chem. Phys.* **68** (1978) 3801 (<https://dx.doi.org/10.1063/1.436185>)
20. R. G. Pearson, *Inorg. Chim. Acta* **240** (1995) 93 ([https://dx.doi.org/10.1016/0020-1693\(95\)04648-8](https://dx.doi.org/10.1016/0020-1693(95)04648-8))
21. P. W. Ayers, R. G. Parr, R. G. Pearson, *J. Chem. Phys.* **124** (2006) 194107 (<https://dx.doi.org/10.1063/1.2196882>)
22. P. W. Ayers, *Faraday Discuss.* **135** (2007) 161 (<https://dx.doi.org/10.1039/B606877D>)
23. R. G. Parr, L. Szentpaly, S. Liu, *J. Am. Chem. Soc.* **121** (1999) 1922 (<https://dx.doi.org/10.1021/ja983494x>)

24. S. B. Liu, in *Chemical Reactivity Theory: A Density Functional View*, P. K. Chattaraj, Ed., Ch. 13, Taylor & Francis, Boca Raton, FL, 2009, p. 179
25. R. Parthasarathi, J. Padmanabhan, V. Subramanian, B. Maiti, P. K. Chattaraj, *Curr. Sci.* **86** (2004) 535
(https://www.currentscience.ac.in/Downloads/article_id_086_04_0535_0542_0.pdf)
26. J. A. War, K. Jalaja, Y. S. Mary, C. Y. Panicker, S. Armakovic, S. J. Armakovic, S. K. Srivastava, C. Van Alsenoy, *J. Mol. Struct.* **1129** (2017) 72
(<https://dx.doi.org/10.1016/j.molstruc.2016.09.063>)
27. I. Fleming, *Frontier Orbitals and Organic Chemical Reactions*, John Wiley and Sons, New York, 1976 (ISBN 978-0-470-74660-8 (H/B), 978-0-470-74659-2 (P/B))
28. E. Scrocco, J. Tomasi, in *Advances in Quantum Chemistry*, P. Lowdin, Ed., Academic Press, New York, 1978 ([https://dx.doi.org/10.1016/S0065-3276\(08\)60236-1](https://dx.doi.org/10.1016/S0065-3276(08)60236-1))
29. A. Grosdidier, V. Zoete, O. Michielin, *Nucleic Acids Res.* **39** (2011) 270
(<https://dx.doi.org/10.1093/nar/gkr366>)
30. R. Ramaswamy, S. Goomeshi Nobary, B. A. Eyford, T. W. Pearson, M. J. Boulanger, *Protein Sci.* **25** (2016) 2297
(<http://www.rcsb.org/pdb/explore/explore.do?structureId=5KLH>)
31. E. F. Pettersen, T. D. Goddard, C. C. Huang, G. S. Couch, D. M. Greenblatt, E. C. Meng, T. E. Ferrin, *J. Comput. Chem.* **25** (2004) 1605 (<https://dx.doi.org/10.1002/jcc.20084>).